



A new Rubidium - Bismuth polyphosphate $\text{RbBi}(\text{PO}_3)_4$: Growth, X-ray single crystal and vibrational study

Khaled JAOUADI*, Tahar MHIRI, Nabil ZOUARI

Laboratoire physico-chimie de l'état solide, Faculté des Sciences de Sfax, BP 1171, 3038 Sfax, Tunisie
khaledjaouadi@yahoo.fr

Laboratoire physico-chimie de l'état solide, Faculté des Sciences de Sfax, BP 1171, 3038 Sfax, Tunisie
taharmhiri@yahoo.fr

Laboratoire physico-chimie de l'état solide, Faculté des Sciences de Sfax, BP 1171, 3038 Sfax, Tunisie
bizrirl@yahoo.fr

ABSTRACT

Solid-solution studies in the ternary $\text{Rb}_2\text{O} - \text{Bi}_2\text{O}_3 - \text{P}_2\text{O}_5$ system, carried out in a search for inorganic materials have a considerable interest mainly for their optical properties, specifically in laser technology, yielded the new compound $\text{RbBi}(\text{PO}_3)_4$. Single-crystal X-ray measurement revealed that $\text{RbBi}(\text{PO}_3)_4$ crystallizes in space group $\text{P2}_1/\text{c}$ with a structural type IV and has lattice parameters $a = 10.430$, $b = 8.984$, $c = 12.967 \text{ \AA}$, $\beta = 126.1^\circ$, $Z = 4$ and $V = 981.6 \text{ \AA}^3$. The all eighteen atoms were located in the asymmetric unit. Refinement using anisotropic temperature factors for all atoms yielded weighted residuals based on F and F^2 values, respectively, of $R_1 = 0.0131$ and $WR_2 = 0.0252$ for all observed reflections. The atomic arrangement can be described as a long chain polyphosphate organization, helical ribbons $(\text{PO}_3)_n$. Two types of infinite chains, with a period of eight PO_4 tetrahedra run along the longest unit-cell directions. Infrared and Raman spectra at room temperature, were investigated, show clearly some characteristics bands of infinite chains structure of PO_4 tetrahedra linked by a bridge oxygen.

Indexing terms/Keywords

Inorganic materials; Crystal structure; X-Ray diffraction; IR spectroscopy; Raman spectroscopy.

Council for Innovative Research

Peer Review Research Publishing System

Journal: Journal of Advances in Chemistry

Vol. 10, No. 7

editorjaconline@gmail.com

www.cirjac.com

1. INTRODUCTION

The structure investigation of the compound $\text{RbBi}(\text{PO}_3)_4$ was performed as part of a research program in condensed phosphates with general formula $\text{M}^{\text{I}}\text{M}^{\text{III}}(\text{PO}_3)_4$ (where M^{I} is a monovalent cation: Li, Na, Ag, K ... and M^{III} is a trivalent cation: Nd, La, Sm, Ce, Y...). The common chemical features of these polyphosphates report that are relatively stable under normal conditions of temperature and humidity [1-7]. These compounds can be kept for many years in a perfect state of crystallinity; they are not water soluble as may be inferred from their estimated molecular weights and they all produce glasses when heated to their melting points [8]. The literature dealing with these compounds was rather confusing for a long time, but it is currently well established that the $\text{M}^{\text{I}}\text{M}^{\text{III}}(\text{PO}_3)_4$ compounds can be classified into seven different structure types, which are usually denoted by the roman numerals I to VII. This nomenclature, first proposed by *Palkina and al* [9] is to-day generally accepted. In addition, many of these compounds are isotypic and some of them are polymorphic. Only the two polyphosphates $\text{KBi}(\text{PO}_3)_4$ (type IV) and $\text{NaBi}(\text{PO}_3)_4$ (type II) have been elaborated in the ternary $\text{M}_2\text{O} - \text{Bi}_2\text{O}_3 - \text{P}_2\text{O}_5$ system and their structures were well discussed by *Jaouadi and al* [10, 11], and up to now, the syntheses and the crystal structure of the other types of polyphosphates existing in this ternary system have been unknown.

Our attempt to prepare new single crystals, in the ternary $\text{P}_2\text{O}_5 - \text{Rb}_2\text{O} - \text{Bi}_2\text{O}_3$ system, from phosphoric acid, bismuth oxide and rubidium carbonate was successful. In fact, this study resulted in a new polyphosphate $\text{RbBi}(\text{PO}_3)_4$ (type IV), whose chemical preparation and crystal structure are presented here. In addition, the titled compound has been characterized by IR and Raman vibrational spectroscopy.

2. EXPERIMENTAL

2.1. Synthesis and characterization

Single crystal of $\text{RbBi}(\text{PO}_3)_4$ was prepared by a flux method. At room temperature, 2.8 g of Rb_2CO_3 and 0.52 g of Bi_2O_3 were slowly added to 2.5 ml of phosphoric acid H_3PO_4 (85 %). The mixture was then slowly heated to 623 K and kept in this temperature for 24 hours. A few days later of decreasing temperature by $40^\circ\text{C}/\text{day}$ to reach 323 K, a colorless, transparent and parallelepiped crystals were separated from the excess phosphoric acid by washing the product in boiling water. Subsequently, a second washing with nitric acid is necessary to eliminate the remaining oxide Bi_2O_3 . Several preparations based on the temperature decreasing speed were necessary to obtain single crystals of dimensions $0.16 \times 0.18 \times 0.08 \text{ mm}^3$ suitable for X-ray study (*Figure 1*).



Figure 1: Photograph of single crystal of $\text{RbBi}(\text{PO}_3)_4$ grown by the flux method

This compound is stable in air and its formula is determined by chemical analysis (*Table 1*) and confirmed by refinement of the crystal structure. In fact, the single crystals already formed correspond to the composition $\text{RbBi}(\text{PO}_3)_4$. It is noted that many preparation with respect to this stoichiometry always led to the same density of crystals ($d_{\text{mes}} = 4.128$). Infrared absorption spectra of suspensions of crystalline powders in KBr were recorded on a Perkin-Elmer 753 spectrophotometer in the $400 - 1500 \text{ cm}^{-1}$ range. Raman spectra of polycrystalline samples scaled in glass tubes were performed by employing an RTI DILOR triple monochromated apparatus using the 514.5 nm line of a spectra-physics argon ion laser.

Table 1: Results of chemical analysis for RbBi(PO₃)₄

	P (%)	Rb (%)	Bi (%)
calculated	20.25	14.00	34.24
experimental	19.42 ^a	13.92 ^b	33.83 ^c

^a Determined by spectrophotometry.

^b Determined by atomic absorption.

^c Determined by ICP method.

2.2. X-ray diffraction and data collection

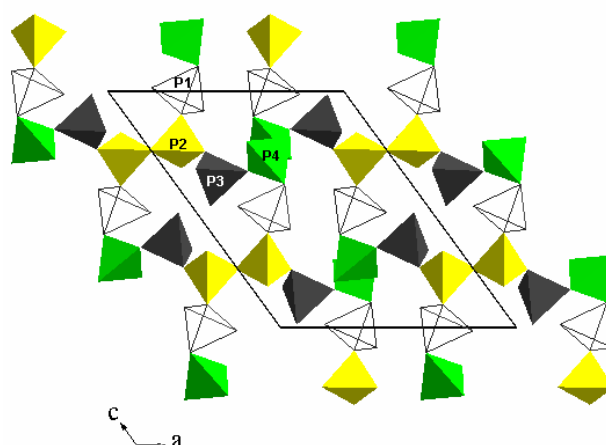
Single-crystal X-ray intensity data were collected at room temperature from an as-synthesized specimen measuring $0.16 \times 0.18 \times 0.08 \text{ mm}^3$ in size. Data were obtained in Mo-K α radiation ($\lambda = 0.71073 \text{ \AA}$) using an Enraf-Nonius Kappa CCD diffractometer. Refinement of the lattice parameters, using the locations of twenty five peaks, revealed RbBi(PO₃)₄ to be monoclinic with lattice parameters $a = 10.430 (5) \text{ \AA}$, $b = 8.984 (4) \text{ \AA}$, $c = 12.967 (4) \text{ \AA}$ and $\beta = 126.1 (3)^\circ$. The raw intensity data were corrected for Lorenz and polarizing effects before proceeding to the refinement of the structure. An empirical absorption correction was performed by using psi-scan method [12]. Atomic scattering factors were taken from the International Tables for X-ray crystallography [13]. 2429 reflections were collected in the whole Ewald sphere for $2.42 \leq \theta \leq 28.68$; $-13 \leq h \leq 11$; $0 \leq k \leq 11$; $0 \leq l \leq 17$. The overage of the equivalent reflections with $I/\sigma(I) > 2$, with respect to the P2₁/c symmetry, gave a final set of 2254 unique observations. The intensities of two standard reflections (3 2 4 and 3 2 $\bar{4}$) were periodically recorded to check the stability of the data acquisition. The remaining data collection parameters, along with some crystallographic data and parameters related to the refinement, are provided in Table2.

Bismuth and rubidium atom positions were located using SHELXS-97 program [14], whereas phosphorus and oxygen atom positions were deduced from Fourier-difference map during the refinement of the structure with an adapted version SHELXL-97 program [15]. There are four formula units in the unit cell and all the atoms are in general positions. The structural graphics were created with ATOMS [16]. The final cycle of refinement leads to the final discrepancy factors $R_1 = 0.0131$ and $WR_2 = 0.0252$. The residual electron density ranged between -1.350 and 1.170 e/\AA^3 , near the Bismuth atom. The final fractional atomic coordinates and equivalent isotropic thermal parameters are given in Tables 3 and 4.

3. RESULTS AND DISCUSSION

3.1. Description of the structure

Views of the structure of RbBi(PO₃)₄, projected along the *b*- and *a*- axes, are illustrated in figures 2 and 3 respectively. As a result of our investigations on polyphosphates, RbBi(PO₃)₄ was shown to be isostructural with KBi(PO₃)₄ [10], KGd(PO₃)₄ [17] and CsGd(PO₃)₄ [18].


Figure 2: The RbBi(PO₃)₄ structure projected along the b axis

From a general point of view, this phosphate could be described as a long chain polyphosphate containing alternating (PO₃)_n chains and (M³⁺, M⁺) cations along the [0 1 1] direction. One can assume that this atomic arrangement is characteristic of this family of polyphosphates [10, 17, 18]. As illustrated in figure 2, the basic structural units are helical ribbons (PO₃)_n, formed by corner-sharing of PO₄ tetrahedra. The ribbons (two per unit cell) run along the longest unit-cell directions, with a period of eight tetrahedral. Every two chains are symmetrical by a twofold axis (Figure 2). These chains are joined to each other by BiO₈ dodecahedra, driving to a tree-dimensional structure, with the Rb⁺ cations located in framework tunnels (Figure 3).

**Table 2: Main crystallographic features, X-ray diffraction data collection parameters and final results for RbBi(PO₃)₄**

I - Crystal Data	
Formula	RbBi(PO ₃) ₄
Formula weight (g/mol)	610.33
Crystal system: Monoclinic	Space group: P2 ₁ /c
a = 10.430 (5) Å	β = 126.1 (3)°
b = 8.984 (4) Å	Z = 4
c = 12.967 (4) Å	V = 981.6 (7) Å ³
d _{cal} = 4.130	μ = 8.606 mm ⁻¹
Habit	colorless
Crystal shape	parallelepiped
Crystal size	(0.16 × 0.18 × 0.08) mm ³
II - Intensity Measurements	
Temperature:	293 (2) K
Diffractometer:	Enraf-Nonius Kappa CCD
Radiation:	λ(Mo-K _α) = 0.71073 Å
Theta range	2.42 – 28.68
Reference reflections (2)	3 2 4; 3 2 4
Measurement area: (h, k, ±l)	-13 ≤ h ≤ 11; 0 ≤ k ≤ 11; 0 ≤ l ≤ 17
Total reflections	2429
III – Structure determination	
Structure solution	Shelxs and Shexl [14, 15]
Corrections	Lorentz and polarization
Empirical absorption correction	ψ scan [12]
Reflection with I/σ (I) > 2	2254
Refined parameters	164
(Δρ) _{min} , (Δρ) _{max} (e/Å ³)	-1.350 and 1.170 e/Å ³
R ₁	0.0131
WR ₂	0.0252
S	1.021

3.1.1. Phosphoric group

The helical (PO₃)_n chains in the RbBi(PO₃)₄ structure, are similar to those of the other alkaline lanthanide polyphosphates [19-21], in which the chains run along the longest unit-cell directions as shown in Figure 2. The polytetraphosphate anion is, as usual in the same group; make up of a chain of eight tetrahedra PO₄ sharing corners. The main interatomic distances and bond angles, in the four independent tetrahedra PO₄ are given in Table 5. As can be seen, the P – O distances may be divided into linking or bridging P – O(Lij) and exterior P – O(Eij) distances (where O(Lij) denotes the O atom that links P_i with P_j and O(Eij) denotes the jth O atom exterior to the chain and bonded to phosphorus P_i) [22]. The linking distances, P – O(Lij), which range from 1.574 to 1.610 Å, are longer than the exterior P – O(Eij) distances, which range from 1.465 to 1.507 Å. The P – O – P angles are understood between 126.2 and 135.4°, which are in good agreement with those usually, met in anions polyphosphates [1-7]. Furthermore, three different types of O – P – O angles co-exist in the PO₄ tetrahedra. The O(L) – P – O(L) angles, mean 99.45°, correspond to the longest P – O bonds, the O(L) – P – O(E) angles have the values expected for a regular tetrahedron and the O(E) – P – O(E) angles correspond to the shortest P – O distances, mean 119.22°, probably induced by mutual repulsion of the non-bridging oxygen atoms (Table5). Nevertheless, the calculated mean distortion indices (DI) [23] corresponding to the



different angles and distances in the independent PO_4 tetrahedra [$\text{DI}(\text{P} - \text{O}) = 0.0378$, $\text{DI}(\text{O} - \text{P} - \text{O}) = 0.0376$ and $\text{DI}(\text{O} \dots \text{O}) = 0.0139$] show that the distortion of the $\text{P} - \text{O}$ distances is greater than that of the $\text{O} \dots \text{O}$ distances. The PO_4 tetrahedra therefore have local C_1 symmetry rather than the ideal $43m$ symmetry [23].

3.1.2. Bismuth coordination

The Bi-atom coordination polyhedra are shown in Figure 4-a, where it can be seen that the irregular eight-coordinate as shows the Bi-O distance. Indeed, these bonds ($\text{Bi} - \text{O}$) range between 2.337 and 2.517 Å (Table 5) with a mean distance 2.427 Å, in agreement with the materials belonging to the $\text{MBi}(\text{PO}_3)_4$ ($\text{M} = \text{K}$ and Na) family which have been synthesized in our laboratory [10, 11]. The eight-coordinate Bi atom, are exterior oxygen atom (OE_{ij}) of the neighboring PO_4 tetrahedra. Although the BiO_8 dodecahedra are considerably distorted, they are isolated from each other in the sense that they do not share any common O atom with the shortest Bi - Bi distance of 5.626 Å. This type of isolation and the coordination number around the Bi-atom is the structural feature that is common to all the polyphosphates. It is to be noted that these dodecahedra BiO_8 are organized in the sense that they formed a zigzag chains according to the $[0\ 1\ 0]$ and $[0\ 0\ 1]$ directions (Figure 4-b).

3.1.3. Rubidium coordination

While the bismuth is in eight-fold coordination, the rubidium atom is surrounded by ten oxygen atoms (Figure. 5-a). This environment is considerably very irregular as can be seen in other rubidium polytetraphosphates [24-26]. In fact, the $\text{Rb} - \text{O}$ distances vary from 2.875 to 3.410 Å with an average of 3.153 Å. The RbO_{10} polyhedra are connected by common corners to $(\text{PO}_3)_n$ chains and by a common edges to bismuth dodecahedra with a Bi-Rb distance of 4.072 Å.

These polyhedra RbO_{10} are bound tow-by-tow to form chains parallel to the $[1\ 0\ 1]$ direction (Figure 5-b). With a comparison of the coordination number around Cs^+ , K^+ , Na^+ and Li^+ in the structures $\text{CsGd}(\text{PO}_3)_4$ [18], $\text{KBi}(\text{PO}_3)_4$ [10], $\text{NaBi}(\text{PO}_3)_4$ [11] and $\text{LiNd}(\text{PO}_3)_4$ [1] respectively, it can be noted that this number decreases from eleven for CsO_{11} polyhedra in the first compound to ten for rubidium atom (RbO_{10}) in the title structure, nine for the potassium (KO_9) and six for the octahedra NaO_6 in the second and the third materials, respectively, while only four for LiO_4 tetrahedra in $\text{LiNd}(\text{PO}_3)_4$ structure. This result can be explained on the basis of the radii of the monovalent cations that $r(\text{Cs}^+) > r(\text{Rb}^+) > r(\text{K}^+) > r(\text{Na}^+) > r(\text{Li}^+)$, so as the number of oxygen per cation in the chemical formula is constant, it is clear that are passes from an open structure of coordination tetrahedra sharing only some edges in $\text{LiNd}(\text{PO}_3)_4$, to a compact framework sharing all edges in $\text{CsGd}(\text{PO}_3)_4$, $\text{RbBi}(\text{PO}_3)_4$ and $\text{KBi}(\text{PO}_3)_4$.

3.2. IR and Raman Spectroscopy Investigations

At room temperature, the compound $\text{RbBi}(\text{PO}_3)_4$ exhibits a monoclinic symmetry with space group ($\text{P}2_1/c$, $Z = 4$). IR and Raman spectra of this compound have been investigated respectively in the frequency range 400 – 1500 and 10 – 1400 cm^{-1} . Figures 6, 7-a and 7-b show IR and Raman spectra of $\text{RbBi}(\text{PO}_3)_4$. All the bands were assigned by comparison with the spectra of $\text{AgGd}(\text{PO}_3)_4$ [19] and $\text{NH}_4\text{Ce}(\text{PO}_3)_4$ [27] at room temperature. The frequencies for the corresponding bands are given in table 6.

The infrared absorption spectra of the compound $\text{RbBi}(\text{PO}_3)_4$, is characterized by the apparition of only one intense band around 1246 cm^{-1} which is assigned to the asymmetric vibration ν_{as} of (PO_2) , this band is observed in the Raman spectra at 1190 cm^{-1} while the weak and strong lines between 1050 and 1150 cm^{-1} in the IR spectra and between 1030 and 1110 cm^{-1} in the Raman spectra are attributed to the symmetric vibration ν_{s} of (PO_2) . The two large bands around 1000 and 930 cm^{-1} in the IR spectra and some weak and broad peaks around 1000 cm^{-1} in the Raman spectra are assigned to the asymmetric vibration ν_{as} of $(\text{P} - \text{O} - \text{P})$. By a comparison with the cyclophosphate $\text{KGdP}_4\text{O}_{12}$ [28], this band appears after 1030 cm^{-1} . We attribute also, the few bands between 730 and 815 cm^{-1} in the IR spectra and at 700, 720 and 810 cm^{-1} in the Raman spectra to the symmetric vibration ν_{s} of $(\text{P} - \text{O} - \text{P})$. All this bands are characteristic of a structure type based on infinite chain of PO_4 tetrahedra bound by a bridge oxygen [21]. We can be note also, that all the bands appears at a frequencies $\leq 200\ \text{cm}^{-1}$ in the Raman spectra are assigned to the translation of the polyphosphate anion $(\text{PO}_3)_4^{4-}$ and to the translation of the cations (Rb^+ and Bi^{3+}).

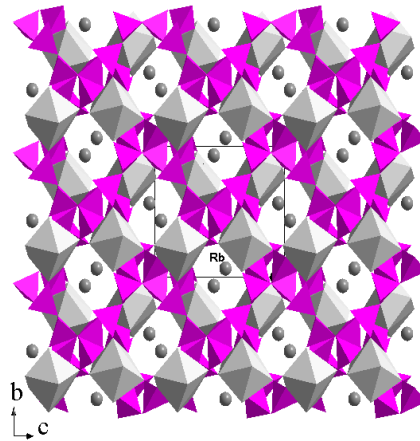


Figure 3: The $\text{RbBi}(\text{PO}_3)_4$ structure projected along the a axis

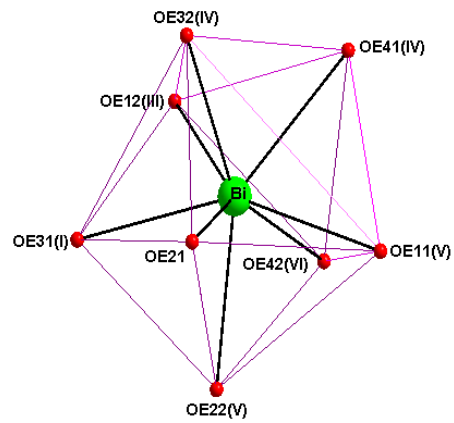


Figure 4 (a): Oxygen environments around the Bi atoms

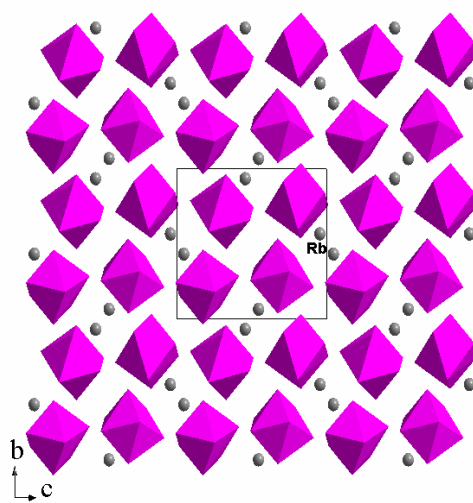


Figure 4 (b): The BiO_x dodecahedrons projected along the a axis

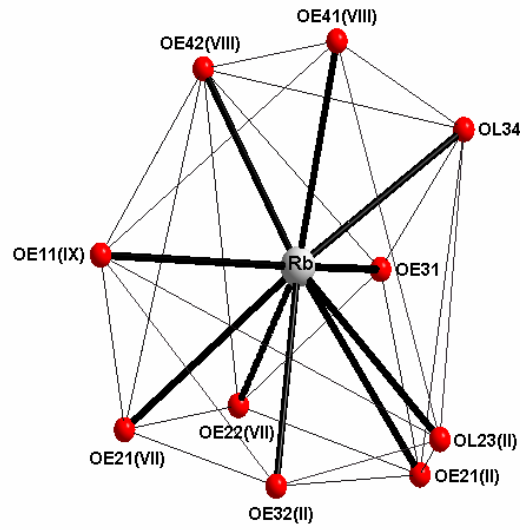


Figure 5 (a): Oxygen environments around the Rb atoms

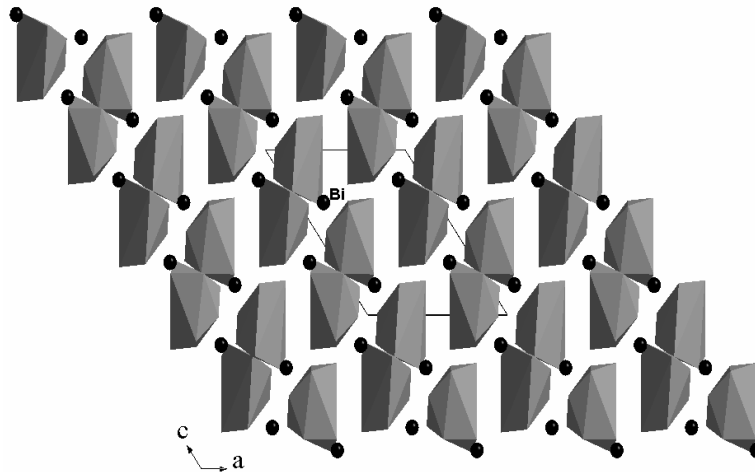


Figure 5 (b): The RbO_{10} polyhedrons projected along the b axis

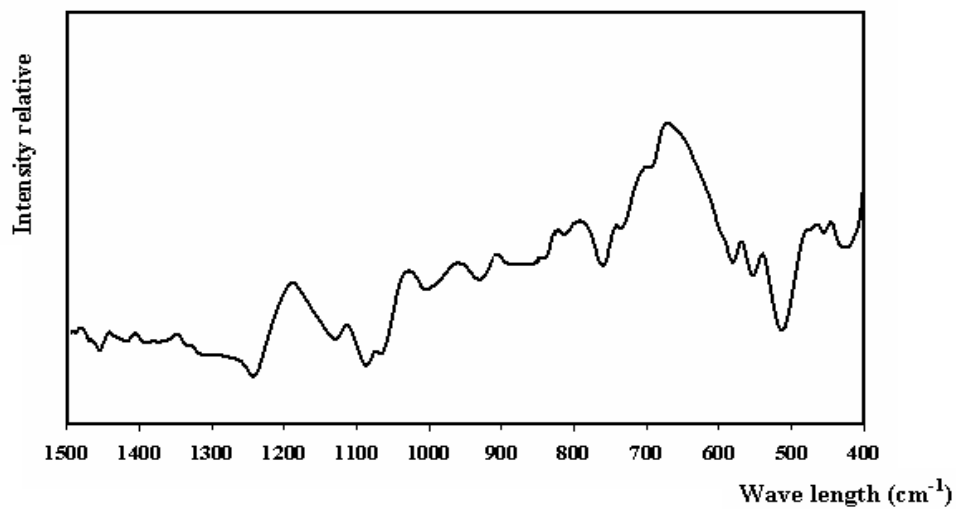


Figure 6: IR spectrum of $\text{RbBi}(\text{PO}_3)_4$ compound at room temperature

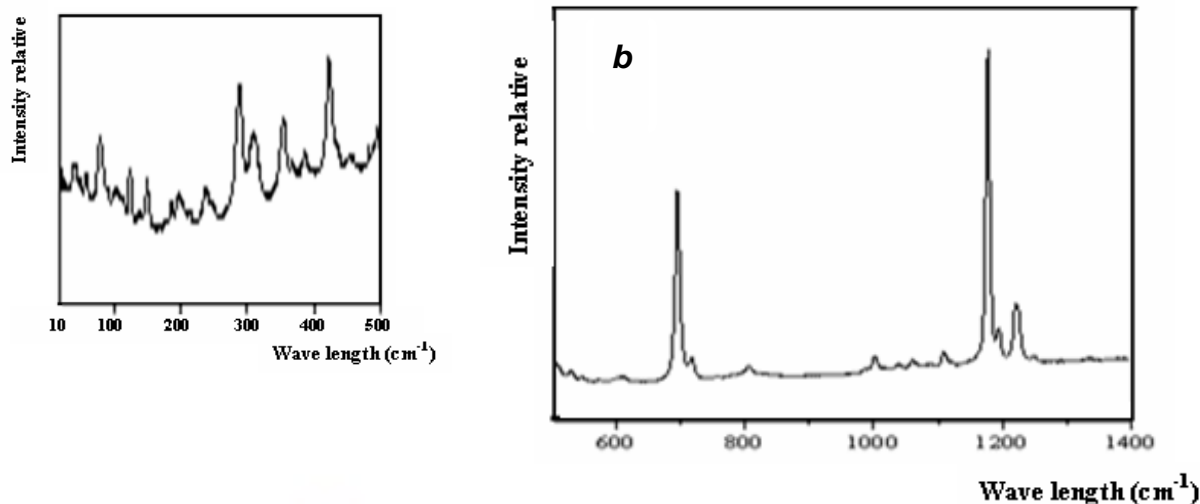


Figure 7: Raman spectrum of $\text{RbBi}(\text{PO}_3)_4$, at room temperature.

(a) in the $10 - 500 \text{ cm}^{-1}$ range,

(b) in the $500 - 1400 \text{ cm}^{-1}$ range

4. CONCLUSION

In the present work, the single-crystal structure of the rubidium bismuth polyphosphate salts $\text{RbBi}(\text{PO}_3)_4$, synthesized by the flux method, have been reported for the first time. The structure analysis confirms that $\text{RbBi}(\text{PO}_3)_4$ is isostructural with $\text{KBi}(\text{PO}_3)_4$, $\text{KGd}(\text{PO}_3)_4$ and $\text{CsGd}(\text{PO}_3)_4$. It crystallizes in monoclinic system (space group $P2_1/c$), with a structural type IV. The main geometrical feature of this structure is the existence of two infinite $(\text{PO}_3)_n$ chains, with a period of eight PO_4 tetrahedra that is to form two dimensional zigzag sheets along the longest unit-cell directions. In this structure, bismuth atoms are in an eightfold coordination, build infinite dodecahedra organized in the sense that they formed a zigzag chains according to the $[0\ 1\ 0]$ and $[0\ 0\ 1]$ directions. The coordination polyhedra of the rubidium atoms are made by ten oxygen atoms. The chains $(\text{PO}_3)_n$ are joined to each other by BiO_8 dodecahedra, driving to a three-dimensional framework structure and delimiting tunnels where are lodged Rb^+ cations. The structural arrangement around the rubidium cations, can favor the appearance of high ionic conductivity at high temperature and this new type of chain has the largest repeat unit ever observed in the polyphosphate domain, so the polarization measurements and Raman spectroscopy versus the temperature are under way and will give more insight into the mechanism of the structural phase transitions for title compound $\text{RbBi}(\text{PO}_3)_4$.

The infrared and Raman spectra at room temperature of the compound $\text{RbBi}(\text{PO}_3)_4$, are characterized by the apparition of a few bands, confirming the presence of infinite chains of PO_4 tetrahedra linked by a bridge oxygen.

5. REFERENCES

- [1] H. Y. P. Hong, *Mat. Res. Bull.* 10 (1975) 635-640.
- [2] H. Koizumi, *Acta Cryst.* B32 (1976) 2254-2256.
- [3] H. Y. P. Hong, *Mat. Res. Bull.* 10 (1975) 1105-1110.
- [4] K. K. Palkina, V. Z. Saifuddinov, V. G. Kuznetsov and N. N. Chudinova, *Dokl. Akad. Nauk SSSR* 237 (1977) 837-839.
- [5] K. K. Palkina, S. I. Maksimova, N. N. Chudinova, N. V. Vinogradova and N. T. Chibiskova, *Izv. Akad. Nauk SSSR Neorg. Mater.* 17 (1979) 110-117.
- [6] K. K. Palkina, S. I. Maksimova and V. G. Kunetsov, *Izv. Akad. Nauk SSSR Neorg. Mater.* 14 (1978) 284-287.
- [7] O. S. Tarasenkova, G. I. Dorokhova, N. N. Chudinova, B. N. Litvin and N. V. Vinogradova, *Izv. Akad. Nauk SSSR, Neorg. Mater.*, 21 (1985) 452-458.
- [8] A. Durif, *Crystal Chemistry of Condensed Phosphates*, Plenum Press, New York (1995) 315-342.
- [9] K. K. Palkina, N. N. Chudinova, B. N. Litvin and N. V. Vinogradova, *Izv. Akad. Nauk SSSR Neorg. Mater.* 17 (1981) 1501-1507.
- [10] K. Jaouadi, H. Naïli, N. Zouari, T. Mhiri and A. Daoud, *Journal of Alloys and Compounds* 354 (2003) 104-114.
- [11] K. Jaouadi, N. Zouari, T. Mhiri and M. Pierrot, *Journal of Crystal Growth* 273 (2005) 638-645.
- [12] A. C. T. North, D. C. Philips and F. S. Matthews, *Acta Cryst.* A39 (1983) 158-166.



- [13] International Tables for X-ray crystallography Vol. C Kluwer, Dordrecht., (1992).
- [14] G. M. Sheldrick, "SHELXS-97", Program for the solution of crystal structures, Univ. of Göttingen, Germany (1990).
- [15] G. M. Sheldrick, "SHELXL-97", Program for crystal structure determination, Univ. of Göttingen, Germany (1997).
- [16] E. Dowly, "ATOMS" for Windows, A Computer Program for Displaying Atomic Structures, Kingsport, TN: Shape Software (1997).
- [17] W. Rekik, H. Naili and T. Mhiri, Acta Cryst. C60 (2004) 50-52.
- [18] H. Naili and T. Mhiri, Acta Cryst. E61 (2005) 204-207.
- [19] H. Naili, H. Ettis and T. Mhiri, Journal of Alloys and Compounds 424 (2006) 400-407.
- [20] M. Rzaigui and N. K. Ariguib., Journal of Solid State Chem. 49 (1983) 391-404.
- [21] V. A. Madir, Yu. I. Krasilov, V. A. Kizel, Yu. V. Denisov, N. N. Chudinova, and N. V. Vinogradova. Izv. Akad. Nauk SSSR Ser. Neorg Mater., 14 (1978) 206-213.
- [22] M. T. Averbuch-Pouchot, A. Durif and J. C. Guttel, Acta Cryst. B32 (1976) 2440-2445
- [23] W. H. Baur, Acta Cryst. B30 (1974) 1195-1199
- [24] H. Ettis, H. Naili and T. Mhiri, Acta Cryst. E62 (2006) 66-68.
- [25] S. I. Maksimova, K. K. Palkina and V. G. Kuznetsov, Dokl. Akad. Nauk SSSR 239 (1978) 1643-1650.
- [26] S. I. Maksimova, K. K. Palkina and N. T. chibiskova, Izv. Akad. Nauk SSSR Neorg. Mater. 22 (1982) 653-657.
- [27] M. Ferid, N. K. Ariguib and M. Trabelsi, Journal of Solid State Chem. 69 (1987) 1-9.
- [28] H. Ettis, H. Naili and T. Mhiri, Crystal Growth and Design 3 (2003) 599-606.

6. ANNEXES

Table 3: Fractional atomic coordinates and temperature factors for $\text{RbBi}(\text{PO}_3)_4$ (Esd given in parentheses)

Atome	x	y	z	U_{eq}
Bi	1.181986(4)	0.223905(4)	0.181211(3)	0.00714(1)
Rb	0.735911(12)	0.066780(12)	0.544890(9)	0.02383(2)
P(1)	0.69516(3)	-0.10757(3)	0.01951(2)	0.00663(4)
P(2)	0.88324(3)	0.09275(2)	0.24022(2)	0.00629(4)
P(3)	0.82121(3)	0.32504(3)	0.36156(2)	0.00602(4)
P(4)	0.52417(3)	0.47305(3)	0.273956(19)	0.00689(4)
O(E11)	0.65519(8)	-0.21241(9)	0.08499(6)	0.01536(13)
O(E12)	0.80533(7)	-0.15656(8)	-0.01332(6)	0.01160(13)
O(L12)	0.75840(8)	0.04685(8)	0.09649(6)	0.01243(14)
O(L14)	0.53866(7)	-0.04569(7)	-0.10617(6)	0.00946(12)
O(E21)	1.01011(9)	0.18062(7)	0.25147(7)	0.01472(14)
O(E22)	0.92777(8)	-0.03694(8)	0.32673(6)	0.01324(13)
O(L23)	0.77336(7)	0.20486(7)	0.25361(6)	0.00962(13)
O(E31)	0.92390(8)	0.25590(7)	0.48855(6)	0.01288(15)
O(E32)	0.86860(8)	0.46295(7)	0.32825(7)	0.01297(13)
O(L34)	0.65293(7)	0.34334(7)	0.33883(6)	0.00838(12)
O(E41)	0.56664(7)	0.58137(7)	0.21052(6)	0.01043(13)
O(E42)	0.36670(7)	0.40443(8)	0.19297(6)	0.01242(14)

$$U_{\text{eq}} = \frac{1}{3} \sum_i \sum_j U_{ij} a_i^* a_j^* a_i a_j$$

**Table 4: Anisotropic displacement parameters (in 10^{-3} \AA^2) for $\text{RbBi}(\text{PO}_3)_4$.**

Atome	U_{11}	U_{22}	U_{33}	U_{23}	U_{13}	U_{12}
Bi	0.01348(1)	0.00264(1)	0.00923(1)	-0.00009(1)	0.00886(1)	0.00016(1)
Rb	0.02448(5)	0.02970(6)	0.01473(4)	-0.00286(4)	0.01012(4)	-0.00527(4)
P(1)	0.01180(11)	0.00481(10)	0.00688(10)	-0.00048(7)	0.00751(9)	0.00013(8)
P(2)	0.01385(10)	0.00066(10)	0.00904(9)	-0.00126(8)	0.00934(8)	-0.00075(8)
P(3)	0.01082(10)	0.00094(10)	0.00903(10)	-0.00071(7)	0.00736(9)	0.00038(7)
P(4)	0.01285(12)	0.00268(10)	0.00849(12)	-0.00072(8)	0.00814(10)	-0.00147(8)
O(E11)	0.0270(3)	0.0083(3)	0.0188(3)	0.0054(3)	0.0179(3)	-0.0017(3)
O(E12)	0.0100(3)	0.0213(3)	0.0076(3)	0.0015(2)	0.0075(3)	0.0015(2)
O(L12)	0.0265(3)	0.0047(3)	0.0088(3)	-0.0062(2)	0.0119(3)	-0.0033(2)
O(L14)	0.0132(3)	0.0070(3)	0.0145(3)	0.0014(2)	0.0117(3)	-0.0022(2)
O(E21)	0.0215(3)	0.0114(3)	0.0196(3)	-0.0061(3)	0.0168(3)	-0.0071(3)
O(E22)	0.0159(3)	0.0056(3)	0.0168(3)	0.0007(2)	0.0088(3)	-0.0008(2)
O(L23)	0.0169(3)	0.0028(3)	0.0117(3)	-0.0058(3)	0.0099(3)	-0.0014(3)
O(E31)	0.0130(3)	0.0151(4)	0.0116(3)	0.0056(2)	0.0078(2)	-0.0020(2)
O(E32)	0.0188(3)	0.0009(3)	0.0285(3)	0.0029(3)	0.0190(3)	0.0014(2)
O(L34)	0.0132(3)	0.0000(3)	0.0151(3)	0.0023(2)	0.0101(3)	0.0010(2)
O(E41)	0.0116(3)	0.0045(3)	0.0134(3)	0.0006(2)	0.0063(3)	-0.0003(2)
O(E42)	0.0117(3)	0.0126(4)	0.0106(3)	-0.0020(3)	0.0053(3)	-0.0052(3)

The anisotropic displacement exponent takes the form $\exp [-2\pi^2 \sum_i \sum_j U_{ij} h_i h_j a_i a_j]$

**Table 5: Bond distances (Å) and angles (°) in RbBi(PO₃)₄ with standard deviations in parentheses**

a. Tetrahedra around P(1)

P(1)	O(E11)	O(E12)	O(L12)	O(L14)
O(E11)	1.483 (7)	2.585 (3)	2.533 (4)	2.513 (3)
O(E12)	119.6 (4)	1.507 (6)	2.535 (3)	2.501 (3)
O(L12)	110.1 (4)	109.0 (4)	1.606 (7)	2.398 (3)
O(L14)	110.2 (4)	107.9 (3)	97.7 (4)	1.579 (7)

b. Tetrahedra around P(2)

P(2)	O(E21)	O(E22)	O(L12)	O(L23)
O(E21)	1.472 (7)	2.549 (3)	2.481 (4)	2.495 (3)
O(E22)	118.8 (4)	1.489 (7)	2.527 (3)	2.532 (4)
O(L12)	109.0 (4)	111.1 (4)	1.574 (6)	2.412 (2)
O(L23)	108.0 (4)	109.5 (4)	98.4 (4)	1.610 (6)

c. Tetrahedra around P(3)

P(3)	O(E31)	O(E32)	O(L23)	O(L34)
O(E31)	1.472 (6)	2.588 (3)	2.514 (2)	2.430 (4)
O(E32)	121.9 (4)	1.489 (7)	2.483 (3)	2.569 (3)
O(L23)	109.9 (4)	107.1 (4)	1.597 (6)	2.446 (2)
O(L34)	104.1 (3)	112.0 (4)	99.5 (3)	1.608 (7)

d. Tetrahedra around P(4)

P(4)	O(E41)	O(E42)	O(L34)	O(L14) ⁱ
O(E41)	1.500 (6)	2.524 (3)	2.527 (3)	2.580 (3)
O(E42)	116.6 (4)	1.465 (7)	2.477 (3)	2.471 (2)
O(L34)	109.6 (3)	108.1 (4)	1.593 (6)	2.497 (3)
O(L14) ⁱ	112.1 (4)	106.9 (4)	102.5 (3)	1.609 (6)

e. Inter-tetrahedral angle

P(1) – O(L12) – P(2)	135.4 (5)
P(2) – O(L23) – P(3)	130.0 (4)
P(3) – O(L34) – P(4)	131.4 (4)
P(1) – O(L14) – P(4) ⁱⁱ	126.2 (4)

a. Polyhedra around Bi

Bi – O(E12) ⁱⁱⁱ	2.337 (6)
Bi – O(E31) ⁱⁱ	2.365 (6)
Bi – O(E32) ^{iv}	2.390 (7)
Bi – O(E22) ^v	2.408 (7)



Bi – O(E42) ^{VI}	2.453 (7)
Bi – O(E21)	2.474 (7)
Bi – O(E41) ^{IV}	2.479 (6)
Bi – O(E11) ^V	2.517 (6)

b. Polyhedra around Rb

Rb – O(E22) ^{VII}	2.875 (7)
Rb – O(E41) ^{VIII}	2.937 (7)
Rb – O(E42) ^{VIII}	2.982 (7)
Rb – O(E31)	2.992 (6)
Rb – O(E32) ^I	3.081 (8)
Rb – O(L23) ^I	3.231 (7)
Rb – O(E21) ^{VII}	3.269 (7)
Rb – O(L34)	3.367 (6)
Rb – O(E21) ^I	3.387 (7)
Rb – O(E11) ^{IX}	3.410 (8)

Symmetry code:

I : $x, -y + \frac{1}{2}, z + \frac{1}{2}$ IV : $-x + 2, y - \frac{1}{2}, -z + \frac{1}{2}$ VII : $-x + 2, -y, -z + 1$ II : $x, -y + \frac{1}{2}, z - \frac{1}{2}$ V : $-x + 2, y + \frac{1}{2}, -z + \frac{1}{2}$ VIII : $-x + 1, y - \frac{1}{2}, -z + \frac{1}{2}$ III : $-x + 2, -y, -z$ VI : $x + 1, y, z$ IX : $x, -y - \frac{1}{2}, z + \frac{1}{2}$



Table 6: Raman and Infrared frequencies (cm⁻¹) and band assignment at room temperature

IR frequencies (cm ⁻¹)	Raman frequencies (cm ⁻¹)	Assignment	
1246	1249	} $\nu_{as}(O-P-O)$	
-	1221		
-	1190		
-	1175		
1143	1107	} $\nu_s(O-P-O)$	
1086	1063		
1068	1037		
1000	1000	} $\nu_{as}(P-O-P)$	
930	-		
812	810	} $\nu_s(P-O-P)$	
758	720		
731	700		
689	609	} $\delta(O-P-O)$	
575	543		
551	527		
510	490		
456	430		
432	420	} $\delta(P-O-P) + \nu Bi-O$	
-	380		
-	350		
-	317		
-	291		
-	239		
-	196		} $T(PO_3)_4^{4-} + T(Rb^+) + T(Bi^{3+})$
-	149		
-	122		
-	73		
-	47		
-	31		